

The Performance of Accelerometers and PVDF Sensors
in Active Structural Vibration Control

Bor-Tsuen Wang¹

國立屏東技術學院學報第三期第81—92頁抽印本

中華民國八十三年六月

The Performance of Accelerometers and PVDF Sensors in Active Structural Vibration Control

Bor-Tsuen Wang¹

ABSTRACT

This paper presents the theoretical analysis of active beam vibration control with the use of accelerometers and PVDF sensors in conjunction with piezoelectric actuators and compares the control effectiveness of the two types of error sensors. A simply-supported beam is considered as the plant. A harmonic point force acts as a disturbance input, and a piezoelectric element bonded to the beam serves as a control actuator. Both accelerometers and PVDF sensors that directly measure the beam responses were individually applied as error sensors. The cost function corresponding to the type of sensors is constructed. The cost function is then to be minimized so as to obtain the optimal input voltages to the piezoelectric actuators. The influence of the location of error sensors on the beam was studied. The vibrating energy spectrum analysis was also performed to evaluate the control effectiveness. An understanding of the control mechanism of various types of sensors is inherent in the design of active structural vibration control system. In particular, this study explores the insight design of intelligent material structures systems which contain actuators and sensors in the sense of distributed.

(Key words: active vibration control, piezoelectric, PVDF)

INTRODUCTION

The research and development of intelligent materials structure system application to structural vibration and acoustic control have been invoked a great deal of interests. The intelligent structures draw much attention not only for their effective controllability but also for their compact structure. Piezoceramic is one of the major components applied to construct the intelligent structures. Bailey and Hubbard [1] used a spatially distributed piezoelectric polymer film actuator for controlling the vibrational modes of a cantilever beam. They found that with the use of distributed parameter actuators and distributed parameter control theory, one can avoid the trade offs due to truncation of the model. Many others also performed their research in applying piezoelectric actuators and sensors for active structural vibration and acoustic control [2-5].

The core of the intelligent structures consists of three components: sensors, actuators and microprocessor-based controller. In contrast to the traditional transducers, such as accelerometers and microphones which are discrete types, the PVDF (polyvinylidene fluoride) films essentially distributed have been widely used as error sensors in active control systems [6]. Researches have

1. Associate professor, Department of Mechanical Engineering, National Pingtung Polytechnic Institute, Taiwan, R.O.C.

(Accepted for Publication on November 15, 1993.)

been conducted to apply such distributed actuators and sensors in wide ranges of applications, especially for structural vibration and sound radiation control. Few literatures focus on the evaluation of distributed types of actuators and sensors in comparison to the traditional transducers. Wang et al. [7] analytically studied the control performance for both traditional force shakers and distributed piezoelectric actuators. Although point force actuators perform better sound radiation control than piezoelectric actuators, piezoelectric actuators can still achieve sufficient control and have more advantages over shakers, such as small volume, low weight and easy implementation.

This paper analytically studies the control performance of the distributed PVDF films and accelerometers as error sensors for active vibration control. A harmonic point force acting on a simply-supported beam is considered as the disturbance. The piezoelectric actuators are employed as the control sources to suppress the beam lateral vibration response. Either accelerometers or PVDF films are applied as error sensors. The cost function corresponding to each type of sensors is then constructed. The linear optimal control theory (LQOCT) is adopted to optimize the input voltages to the piezoelectric actuator so as to minimize the cost function. The performance of PVDF film sensors is evaluated for various locations and excitation frequencies. Finally, a comparison of the control effectiveness between the accelerometers and PVDF films in terms of vibrating energy is made. This work gives an understanding of control mechanism for various types of sensors. Therefore, one can properly selecting the error sensors in the design of intelligent materials structure systems for active structural vibration and acoustic control.

THEORETICAL ANALYSIS

Lateral Vibration of Uniform Beam

Consider a uniform simply-supported beam with length of L , as shown in Figure 1, the equation of motion can be obtained as follow:

$$E_b I \frac{\partial^4 y}{\partial x^4} + \rho_b b t_b \frac{\partial^2 y}{\partial t^2} = p(x,t) \quad (1)$$

where E_b is the Young's modulus of the beam; I the moment of inertia; ρ_b the beam density; t_b the beam thickness; b the beam width; $p(x,t)$ the force function. Note that the damping effect is assumed small and can be neglected for simply application. The boundary conditions for a simply-supported beam are

$$M(0,t) = M(L,t) = E_b I \frac{\partial^2 y}{\partial x^2} = 0 \quad (2)$$

$$y(0,t) = y(L,t) = 0 \quad (3)$$

For free vibration analysis, i.e., $p(x,t) = 0$, the natural frequencies can be found to be

$$\omega_n = (n \pi)^2 \sqrt{\frac{E_b I}{\rho_b b t_b L^4}} \quad (4)$$

The general form of beam lateral displacement, while the beam is subjected to harmonic force inputs, can be written as the follow:

$$y(x,t) = e^{i\omega t} \sum_{n=1}^{\infty} W_n \sin \alpha_n x \quad (5)$$

where

$$\alpha_n = \frac{n\pi}{L} \quad (6)$$

$$W_n = \frac{P_n}{\rho_b b t_b (\omega_n^2 - \omega^2)} \quad (7)$$

Here ω is the excitation frequency; α_n is the modal number; W_n is the modal amplitude; and P_n is the modal force depending on the forms of external forces.

Point Force Excitation:

For a harmonic point force with the amplitude of F located at x_f acting on the beam, the force function, $p(x,t)$, can be written as follow:

$$p(x,t) = F \delta(x-x_f) e^{i\omega t} \quad (8)$$

The Delta function, $\delta(x)$, is employed to represent the location of the point force. The modal force, P_n^f , due to the point force excitation is given as follow:

$$P_n^f = \frac{2F}{L} \sin \alpha_n x_f \quad (9)$$

where the superscript f signify the point force.

Piezoelectric excitation:

For an actuator consisting of two identical piezoceramic patches bonded symmetrically on the two opposite beam surfaces and activated 180° out-of-phase, the equivalent external forces can be derived as follow [8]:

$$p(x,t) = M_{eq} [\delta'(x-x_1) - \delta'(x-x_2)] e^{i\omega t} \quad (10)$$

where

$$M_{eq} = C_0 \Lambda = \frac{t_b^2 E_b}{6} K b_a \Lambda \quad (11)$$

$$K = \frac{6}{6 + \Psi} \quad (12)$$

$$\Psi = \frac{E_b t_b}{E_a t_a} \quad (13)$$

$$\Lambda = \frac{d_{31}}{t_a} V \quad (14)$$

$C_0 \Lambda$ is the equivalent moment induced by the piezoelectric patches attached to the top and bottom of the beam and excited 180° out-of-phase. Λ is the strain induced by an unconstrained piezoelectric layer of thickness, t_a , when a voltage V is applied along its polarization direction, while d_{31} is the piezoelectric dielectric strain constant. Ψ is the effective stiffness ratio [9]. The

resultant force is, in fact, the concentrated moments acting on the both edges of piezoelectric patches represented by the first derivative of Delta function. The corresponding expression of modal force for piezoelectric excitation, P_n^c , can be derived [8] as follow:

$$P_n^c = \frac{2M_{e3}}{L} \alpha_n (\cos \alpha_n x_1 - \cos \alpha_n x_2) \quad (15)$$

where x_1 and x_2 are the coordinates of the piezoelectric actuator, and the superscript c signify the control force.

PVDF sensors' equations

For a PVDF film arranged as shown in Figure 1, the shape function can be expressed as follow:

$$\Gamma(x) = u(x-x_{s1}) - u(x-x_{s2}) \quad (16)$$

where $u(x)$ is the step function; x_{s1} and x_{s2} are the coordinates of the PVDF film. The sensor's equation can then be derived as follows [10]:

$$q(t) = \frac{t_b + t_s}{2} b_s e_{31} \int_0^L \Gamma(x) \frac{\partial^2 y}{\partial x^2} dx$$

where b_s is the sensor width; t_s the sensor thickness; e_{31} the piezoelectric field intensity constant. By substituting and integrating over the beam length,

$$q(t) = e^{i\omega t} \left(\frac{t_b + t_s}{2} e_{31} b \right) \sum_{n=1}^{\infty} \alpha_n W_n (\cos \alpha_n x_{s2} - \cos \alpha_n x_{s1}) \quad (18)$$

The generated voltages can then be expressed as:

$$V(t) = \frac{q(t)}{\epsilon A} t_s \quad (19)$$

where ϵ is the permittivity of PVDF films; A is the sensor area. It is noted that the generated voltage is proportional to the slope difference between the two edges of a PVDF film.

LQOCT for PVDF sensors

For N_s PVDF sensors, the cost function can be defined as the sum of the mean square voltages measured from the PVDF films:

$$\Psi_v = \sum_{j=1}^{N_s} |V_j|^2 \quad (20)$$

The linear quadratic optimal control theory (LQOCT) can then be applied to minimize the cost function so as to find the optimal control voltages input to the piezoelectric actuators. The full analysis can be referred to [8] and omitted here for brevity. The vibrating energy of the beam can be expressed as follow:

$$\Phi_w = \int_0^L |y|^2 dx \quad (21)$$

which can be used as an index to evaluate the control performance.

ANALYTICAL RESULTS AND DISCUSSIONS

A steel beam with length of 0.38m, width of 0.04m, and thickness of 2mm is used in the simulations. The first few natural frequencies are 33.2 Hz, 128.8 Hz, 289.9 Hz, 515.4 Hz, 805.3 Hz and 1159.6 Hz. It is noted that no damping was included in the following analysis. In order to calculate the beam response, it was necessary to truncate the modal sums in Equation (5). Upon consideration of computing time and accuracy, the first 20 modes were considered, and it was found to provide sufficient convergence of series.

The following results consist of the displacement distribution of beam vibrational amplitude plotted along the beam length. The results are normalized by the largest amplitude obtained in each case. The amplitude of the point force disturbance input is fixed at $F=0.1\text{N}$ located at $x_f=0.067\text{m}$. The piezoceramic patch located at $x_1=0.285\text{m}$, $x_2=0.3485\text{m}$ is G-1195 [12], and the PVDF film is LDT-28 μk [13].

First mode excitation

Figure 2 shows the beam displacement distribution for different location of PVDF sensor under active control at $f=33\text{Hz}$, i.e., near the first resonance mode. The arrangement of the piezoelectric actuator and PVDF sensors is depicted on the top of the figure. The solid line, as expected shown the first mode response, represents the beam response due to the disturbance alone. With control in conjunction with the use of the piezoelectric actuator and PVDF film sensors at different location denoted from P1 to P4, the residual response of the beam is shown in Figure 2. One can observe that the residual response near the PVDF film maintain a constant slope, because the PVDF sensors measure the slope difference between the two edges of the PVDF film, and the LMS control algorithm tends to minimize the slope. As varying the location of PVDF films, the residual response has slightly different from each other. As shown, the reduction of vibrating power has the highest value (27.9 dB) for the PVDF film at P4 location. Note that P4 is not the optimal location. The residual response reveals a distorted second mode shape. Therefore, in order to achieve better control, an idea is to change the modal response to a higher mode which generally has smaller energy. The location of PVDF error sensors affects the control performance. An optimization procedure may be needed to search for the optimal location of PVDF films; however, it is out of the content of this paper.

In order to compare the performance between PVDF and accelerometers sensors, the accelerometer is assumed to be located at the central location of a PVDF film corresponding to the cases in Figure 2. The system arrangement is shown on the top of Figure 3. One can observe that the displacement at the accelerometer location is driven

to be zero due the effect of LMS control algorithm. It should be noted that although the A3 location is not the optimum, the A3 accelerometer, located near the point having the largest response without control, gives the best control performance among all. Wang [8] had previously shown a optimization procedure to determine the optimum location of the accelerometer. In comparison with the PVDF sensors (results shown in Figure 2), the accelerometer generally perform better vibration control, and the selection of the sensor's location is important of achieving efficient control. The control mechanism for both the accelerometer and PVDF sensors have inherent differences due to their different measuring quantities. The accelerometer measures the acceleration at its location, while the PVDF sensor measures the slope difference between the two edges of the PVDF film.

Second mode excitation

Figures 4 and 5 respectively show the beam displacement distribution for different location of PVDF and accelerometer sensors under active control at $f=130\text{Hz}$, i.e., near the second resonance mode. The system arrangement is also shown on the top of the figures. In Figure 4, the PVDF sensor at P2 location gives more reduction of vibrating energy (33.3 dB) than any others. The residual response become a third-mode-like response. Again, this gives an idea of control approach to suppress the lower mode response leading to a higher residual mode, as known modal restructuring [11]. The similar control mechanism can be found for the use of accelerometers in Figure 5. For both the accelerometer (A3) and PVDF (P3) sensors centrally and symmetrically located at the beam, the control failed due to poorly located sensors. The PVDF and accelerometer sensors should not be centrally or symmetrically located near the nodal point. Among the cases shown, the P2 PVDF sensor achieving 33.3 dB reduction of vibrating energy gives the best control performance among all, although the P2 is not the optimum. In summary, with the proper selection of the location of PVDF sensor. The PVDF film sensor can achieve sufficient control as well as the accelerometer. PVDF sensors, integrated with structures, also possess many advantages over accelerometers, such as small size, low cost, and easy implementation.

Vibrating energy spectrum analysis

In order to evaluate the performance of both PVDF and accelerometer sensors over a wide range of frequencies excitation, the centrally located accelerometer (A3) and PVDF film (P3) are chosen to compare the reduction of vibrating energy. Figure 6 shows the scaled vibrating energy over the frequency range up to 1000 Hz, in which the first five resonance modes are included. The accelerometer achieves better control near the first resonant mode than PVDF. For off-resonant excitation between the first and second or the second and third modes, the PVDF sensors works slightly better than the accelerometer. This conclude that the PVDF film has more flexibility to adjust itself for control than the accelerometer of off-resonance excitation. For higher mode exciting, the performance of the PVDF and accelerometer sensors are about the same.

CONCLUSIONS

PVDF film sensors are shown effective for beam vibration control. The control mechanisms for both accelerometers and PVDF film sensors are analytically shown different from each other due to their physical characteristics. The accelerometers performs slightly better control than the PVDF film sensors; however, the PVDF films have more advantages over the accelerometers, such as small volume, low weight and easy implementation. In particular, the use of compact distributed types of transducers, such as piezoelectric actuators and PVDF films sensors, is the essential concept of intelligent materials structure systems. This work can be useful for the design of intelligent materials structure systems.

REFERENCES

1. Bailey, T., and J. E. Hubbard, 1985, "Distributed Piezoelectric-Polymer Active Vibration Control of a Cantilever Beam," AIAA Journal of Guidance and Control, Vol. 6, No. 5, pp. 605-611.
2. Dimitriadis, E. K., C. R. Fuller, and C. A. Rogers, 1991, "Piezoelectric Actuators for Distributed Vibration Excitation of Thin Plates," Journal of Vibration and Acoustics, Vol. 113, pp. 100-107.
3. Wang, B.-T., R. A. Burdisso, and C. R. Fuller, 1991, "Optimal Placement of Piezoelectric Actuators for Active Control of Sound Radiation From Elastic Plates," present in Noise-Con 91, Tarrytown, New York, July.
4. Wang, B.-T., E. K. Dimitriadis, and C. R. Fuller, 1991, "Active Control of Structurally Radiated Noise Using Multiple Piezoelectric Actuators," AIAA Journal, Vol. 29, No. 11, pp. 1802-1809.
5. Wu, W. Z., and M. J. Tzeng, 1991, "Structural Dynamics and Vibration Control of Intelligent Materials," Proceeding of the fifteenth National Conference on Theoretical and Applied Mechanics, pp. 1759-1766.
6. Buke, S. E., and J. E. Hubbard, 1991, "Distributed Transducer Vibration Control of Thin Plates," Journal of Acoustical Society of America, Vol. 90, No. 2, pp. 937-944.
7. Wang, B.-T., C. R. Fuller, and E. K. Dimitriadis, 1991, "Evaluation of Active Control of Noise Transmission Through Rectangular Plates Using Multiple Piezoelectric or Point Force Actuators," Journal of Acoustical Society of America, Vol. 90, No. 5, pp. 2820-2830.
8. Wang, B.-T., 1992, "A Dynamic Simulation of Hybrid Active and Passive Control of Structural Vibration," NSC Report, NSC81-0401-E-020-501.
9. Crawley, E. F., and J. de Luis, 1987, "Use of Piezoelectric Actuators as Elements of Intelligent Structures," AIAA Journal, Vol. 25, No. 10, pp. 1373-1385.
10. Lee, C. K., and F. C. Moon, 1990, "Modal Sensors/Actuators," Journal of Applied Mechanics, Vol. 57, pp. 434-441.
11. Fuller, C. R., C. H. Hansen, and S. D. Snyder, 1990, "Active Control of Sound Radiation From a Rectangular Panel by Sound Sources and Vibration Input: an Experimental Comparison," to appear in Journal of Sound and Vibration.
12. Piezo Systems, Inc., 1990, Product Catalog.
13. Pennwalt Corporation, 1990, Piezo Film Sensor Application Notes.

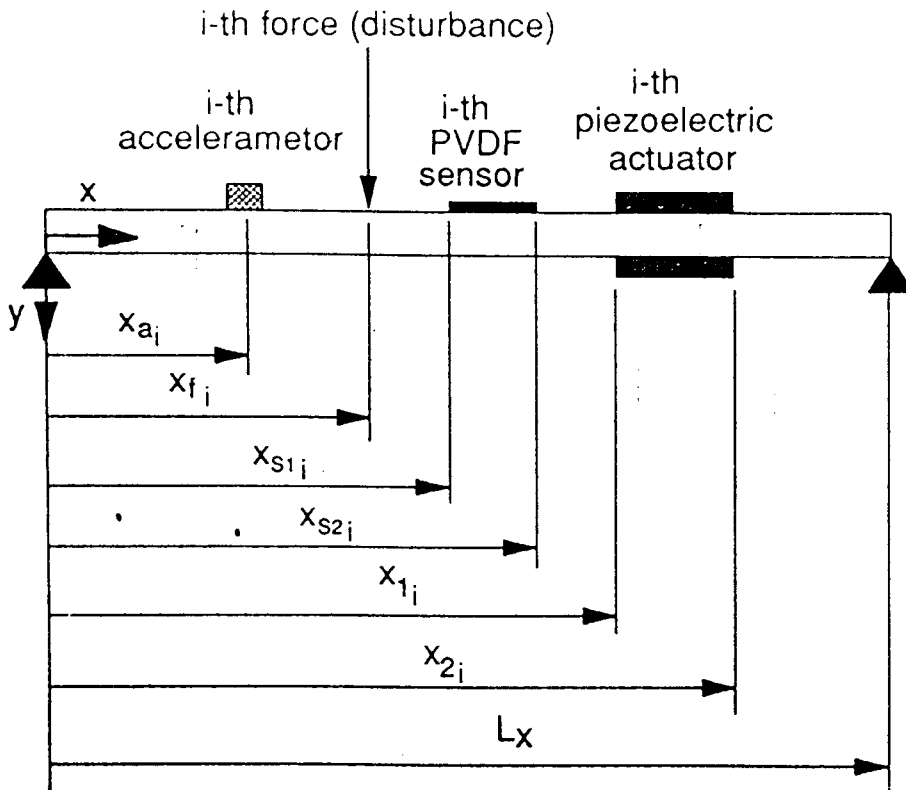


Figure 1. The arrangement and coordinates of simply-supported beam

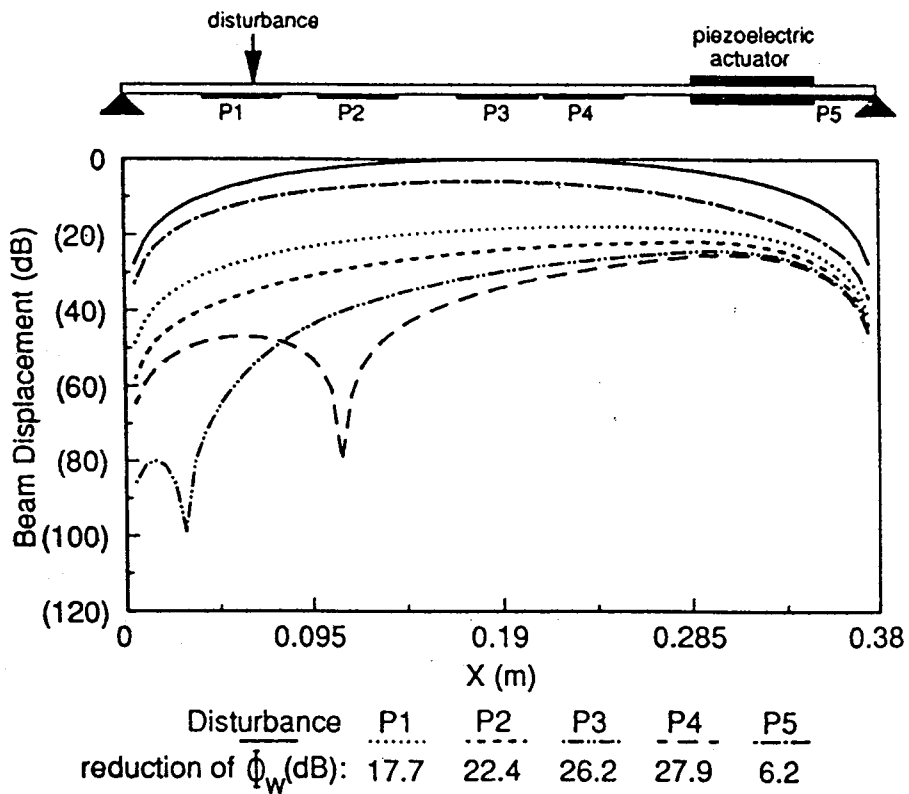


Figure 2. Displacement distribution of the beam for different location of PVDF sensors under active control, $f=33$ Hz

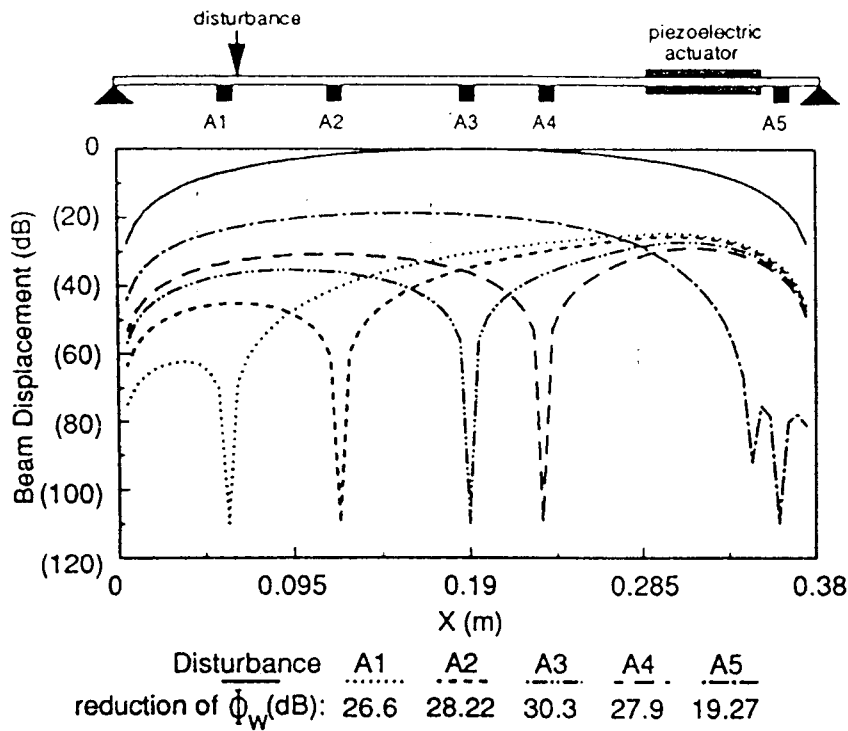


Figure 3. Displacement distribution of the beam for different location of accelerometer sensors under active control

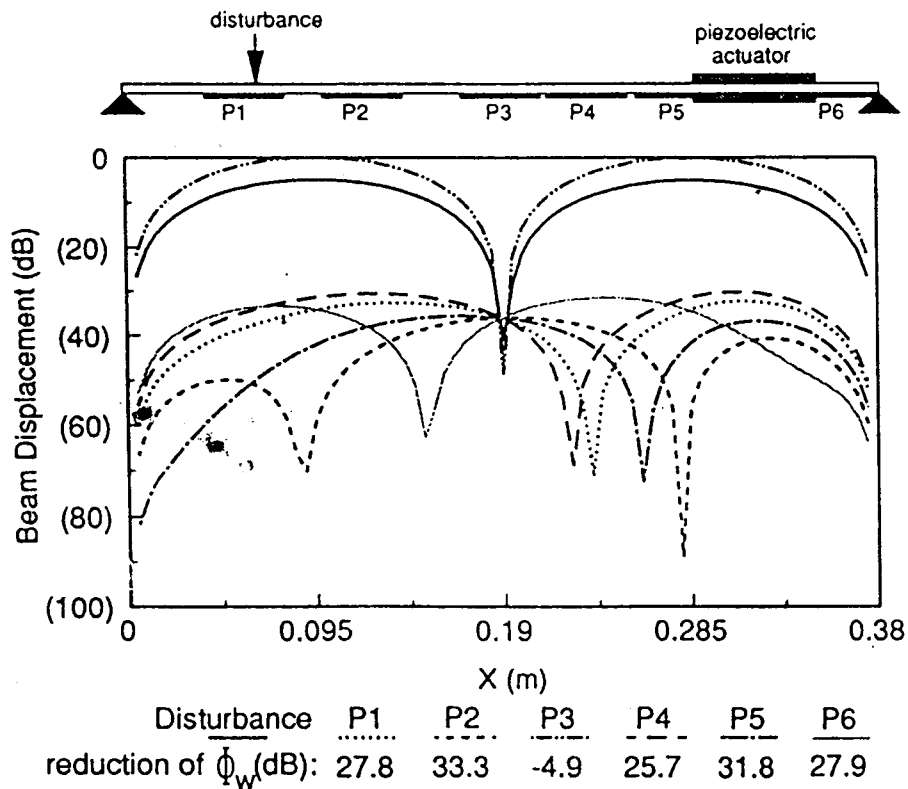


Figure 4. Displacement distribution of the beam for different location of PVDF sensors under active control, $f=130\text{Hz}$

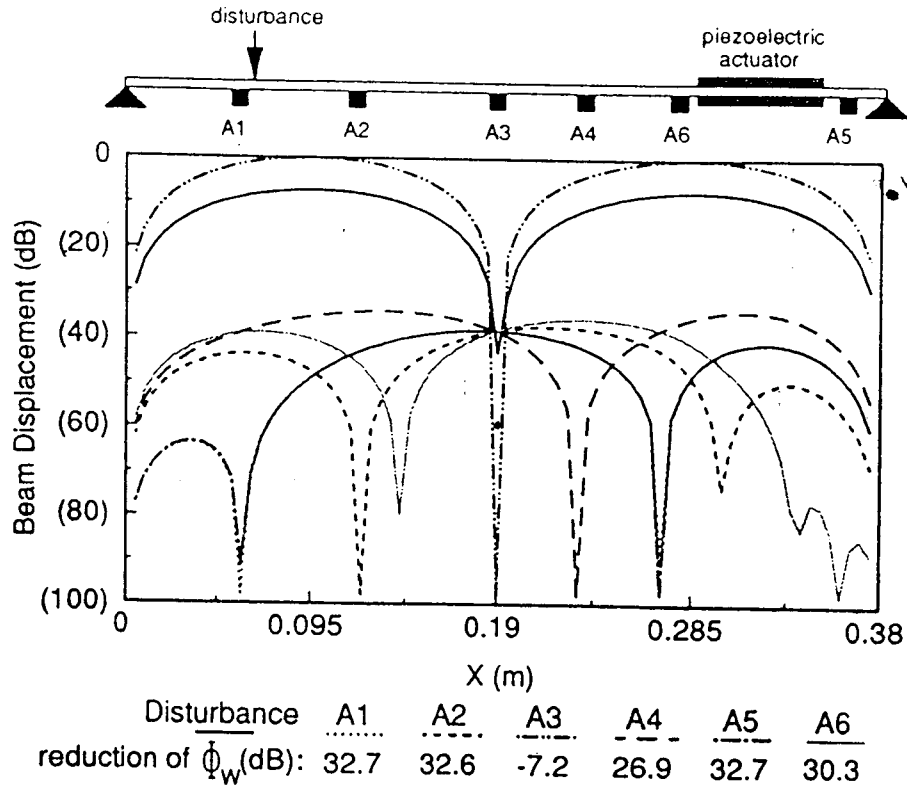


Figure 5. Displacement distribution of the beam for different location of accelerometer sensors under active control, $f=130\text{Hz}$

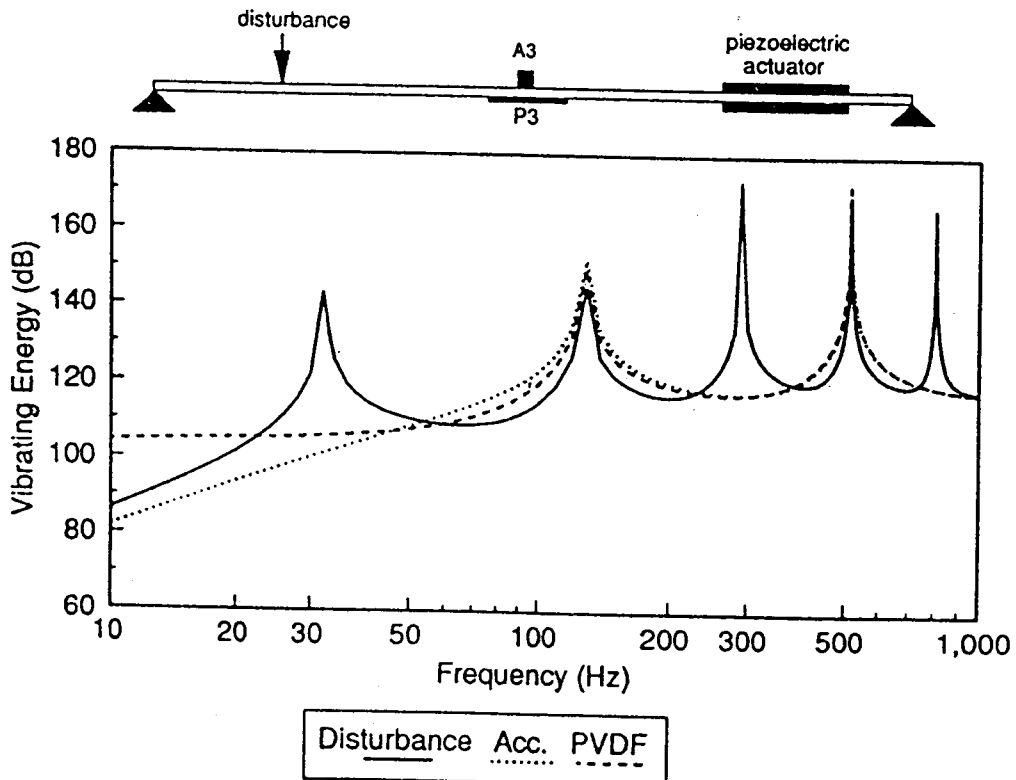


Figure 6. Spectrum analysis for the A3 accelerometer and the P4 PVDF film sensor

加速規與壓電薄膜感應器在主動結構振動控制之效果

王 栢 村¹

摘 要

本篇論文探討樑之主動控制分析，應用壓電材料為致動器，以加速規及壓電薄膜為感測器，並比較兩種感測器之控制效果。系統為一簡支樑，簡協點力為干擾源，壓電材料黏著於樑上作為控制源，加速規及壓電薄膜分別作誤差感應器置於樑上感測樑之反應。建立相對應於感測器之成本函數，將此成本函數最小化以求得壓電致動器之最佳輸入電壓，探討誤差感測器位置之影響，並作振動能量之頻譜分析，以評估控制效果。在主動結構控制系統之設計，必須了解不同感測器之控制情形，本論文特別引導了包含均佈型致動器與感測器之智慧材料結構系統的設計。

(關鍵詞：主動振動控制，壓電材料，壓電薄膜)

-
1. 國立屏東技術學院機械工程技術系副教授。
(本文於中華民國八十二年九月廿五日收稿)